

https://dspace.org/

The role of the particle size and distribution and its allied physical characteristics on the transportation of medium and dense phase slurries in South Africa

Verkerk, Cornelius Gerardus

2011-05-24
http://hdl.handle.net/10539/9901

Downloaded from a DSpace repository. https://dspace.org/

The role of the particle size and distribution and its allied physical characteristics on the transportation of medium and dense phase slurries in South Africa.

CORNELIUS GERARDUS VERKERK

A thesis submitted to the Faculty of Engineering, University of the Witwatersrand, Johannesburg, in fulfillment of the requirements for the degree of Doctor of Philosophy.

Johannesburg, September 1990

[v. 2]

9. ANALYSIS OF THE MEDIUM PHASE SLURRY PUMPING TESTS

9.1 Introduction

The rheological analysis of the different products in Chapter 7 has indicated that non-Newtonian characteristics are prevalent at low concentrations (C_v = 20-45%). This characteristic is more defined the finer the material.

Medium phase slurries are investigated in this section from the point of view of:

1) The influence of the particle size distribution and indicated non-Newtonian characteristic on the pressure gradients of the mixtures.
2) The presence of minimum deposit velocities and the influence of particle size and concentration on this characteristic.
3) The influence of the particle size and concentration on the settling and restart characteristics of these slurries.
4) The practical limitations of adding coarse material to a fine material carrier and the influence on the pressure gradient and the critical deposit velocities.

The following materials were included in the investigation and form part of systems planned and in operation.

1) Tailings 14
2) Tailings 15
3) HMC
4) PFA 2/and BBA
5) Tails 16
6) Tails 17

The salient features of the products tested are included in the following Table (9.1).

Table 9.1 Salient Dimensional and Material Characteristics of the Products Tested

Product	Dimensions (μm)					Material Characteristics	
	d_{10}	d_{40}	d_{50}	d_{60}	d_{90}	Solids s.g.	$\varnothing_{max}$ (%)
Tails 14	17,2	142,2	169,4	196,1	344,1	3,021	52,2
Tails 15	175,9	242,2	264,0	285,2	404,6	2,710	
Tails 16	87,2	135,8	149,9	163,0	202,5	2,680	
Tails 17	39,5	138,3	156,9	176,6	274,0	2,733	47,6
HMC	105,7	130,8	139	147,4	272,5	4,400	55,9
PFA 2	4,8	23,0	32,1	45,8	127,2	2,230	46,1
BBA	101	353,4	503,8	757,0	4283	2,360	38,9

The tailings products are transported in backfilling and gold reclamation systems. The heavy medium concentrate (HMC) is transported from a floating dredge/concentrator to a cyclone and temporary dump, while the PFA and BBA is transported from a coal fired power station to settling dams a few kilometers away from the power station.

The definition of a medium phase slurry is loosely applied although in this report it indicates the maximum range of concentrations that can be transported with a centrifugal pump without a major change in the pump efficiency.

The slurries were all tested in the dilute and medium phase test facility, in pipe sizes ranging from 50 to 200 mm.

The actual pipe size depending on the particular application and tonnage requirements of the slurry being tested.

9.2 Tails 14

Pipeline tests were conducted with these tailings up to a concentration of C_w = 73,1% in a 52 mm and 158 mm pipeline. Prior to the slurry tests, water was pumped through both pipelines to ascertain their individual relative roughnesses.

The k/d value for the steel 52 mm pipe was found to be equal to 0,0009 (Fig. 9.1). This value was obtained by successive iterations of the Colebrook-White equation which is utilized as the basis of the modern day friction factor chart[1]. The value of k/d obtained in this way corresponds with the value quoted in fluid dynamics handbooks[1] for the roughness of commercial steel.

The water gradient tests for the 158 mm pipeline and the corresponding curve for the derived k/d value is illustrated in Fig. 9.2. The 158 mm pipe is galvanized and thus a higher roughness ratio than for the equivalent commercial steel pipe can be expected. The value corresponding to the experimental results is 0,001. It should be borne in mind that the relative roughness gradients measured are for a 40 m length of pipe that includes 6 welded flange joints.

The 52 mm pipe slurry friction gradient results are illustrated in Fig. 9.3 in terms of kPa/m and in Fig. 9.4 in terms of m_{sl}/100m. It is interesting to note that the friction gradient (Fig. 9.4) for flowrates larger than

11,5 m^3/hr is less than the water gradients for the lower concentration slurries and only slightly higher for the slurry with C_w = 65,98%.

The friction gradient results for the 158 mm pipe are illustrated in Fig. 9.5 in terms of kPa/m and in Fig. 9.6 in terms of m_{sl}/100m. Similar characteristics to those occurring with the 52 mm results (APPENDIX X) are prevalent in the larger pipe.

The relatively coarse nature of the tailings resulted in a critical deposit velocity being observed in both pipes. The velocity measured being dependent on the pipe size and average solids concentration prior to deposition on the pipe floor.

The approximate minimum deposit velocity is obtained by observing the flow of slurry through transparent viewing sections in each pipeline. As the exact demarcation between the various flow regimes is difficult to pinpoint, the absolute magnitude of the critical deposit velocity cannot be accurately determined by purely visual means. The visual observation is also influenced by the subjectiveness of the person observing.

To obtain the approximate deposit velocity, the conditions within the pipeline are monitored for each pump speed. The conditions within the pipelines and the average flowrates measured are contained in Table 9.2.

The 58 mm test results indicate a decreasing value of critical deposit velocity as the C_w increases from 47,3% to 60,8%. A similar deposit velocity in the region of 1,12 m/s occurs for both C_w's of 60,8 and 65,98%.

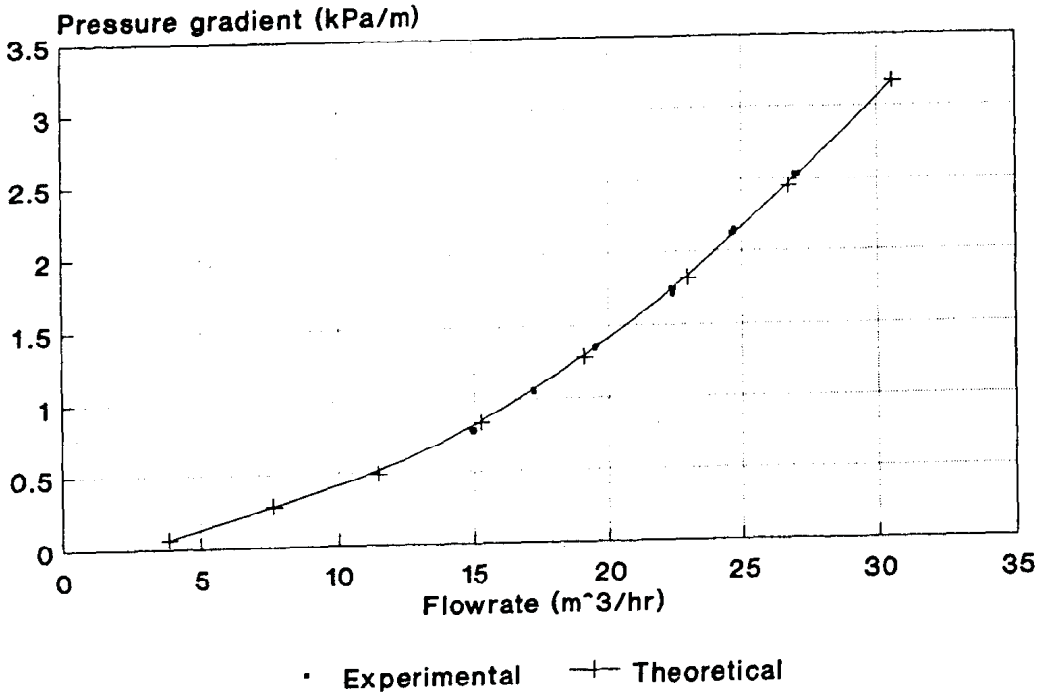

Figure 9.1 Clean water friction gradients (D = 52mm)

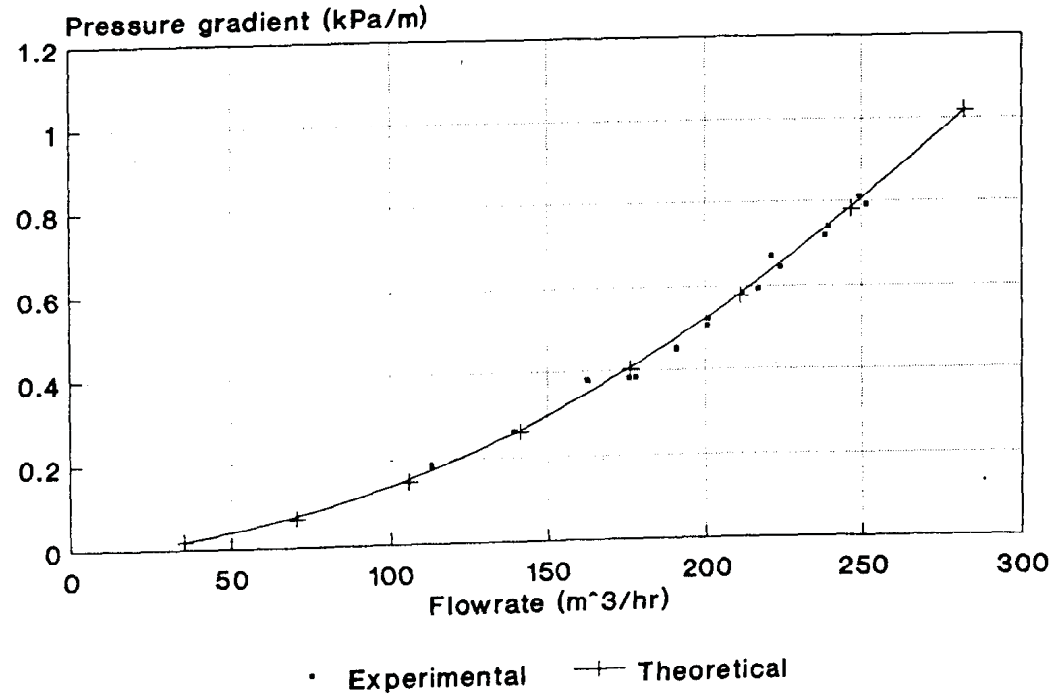

Figure 9.2 Clean water friction gradients (D = 158mm)

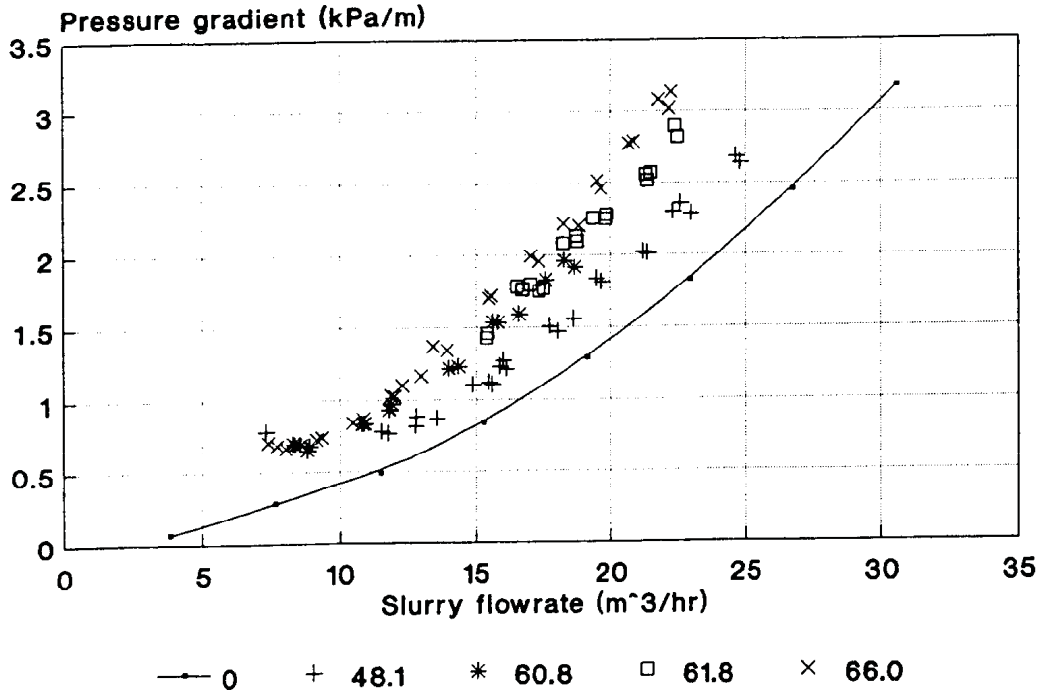

Figure 9.3 Slurry friction gradients (D = 52mm)

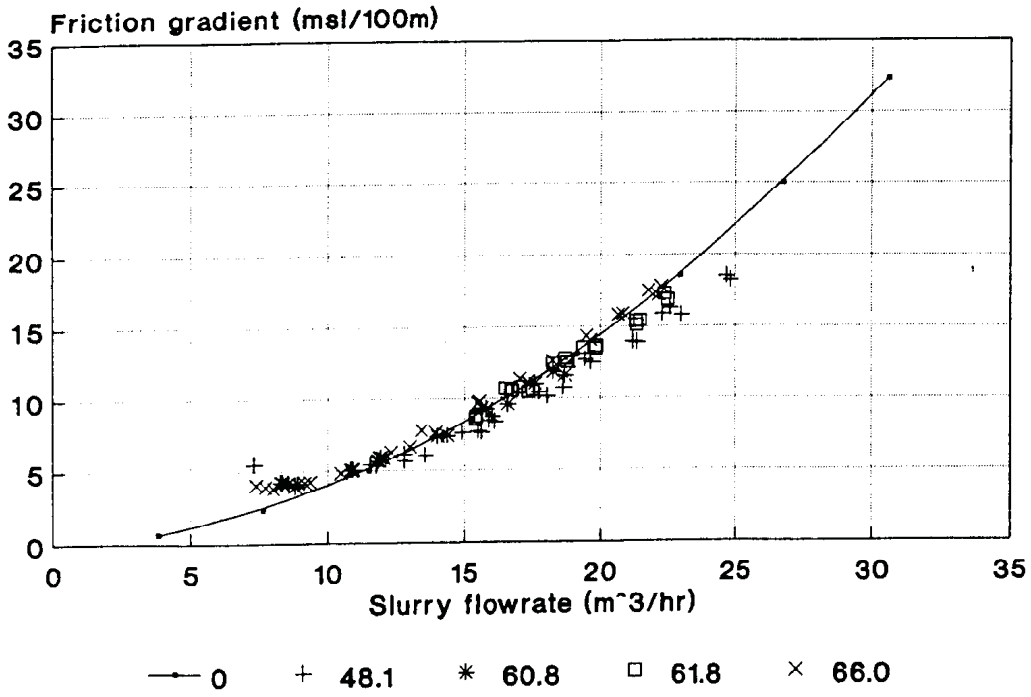

Figure 9.4 Slurry friction gradients (D = 52mm)

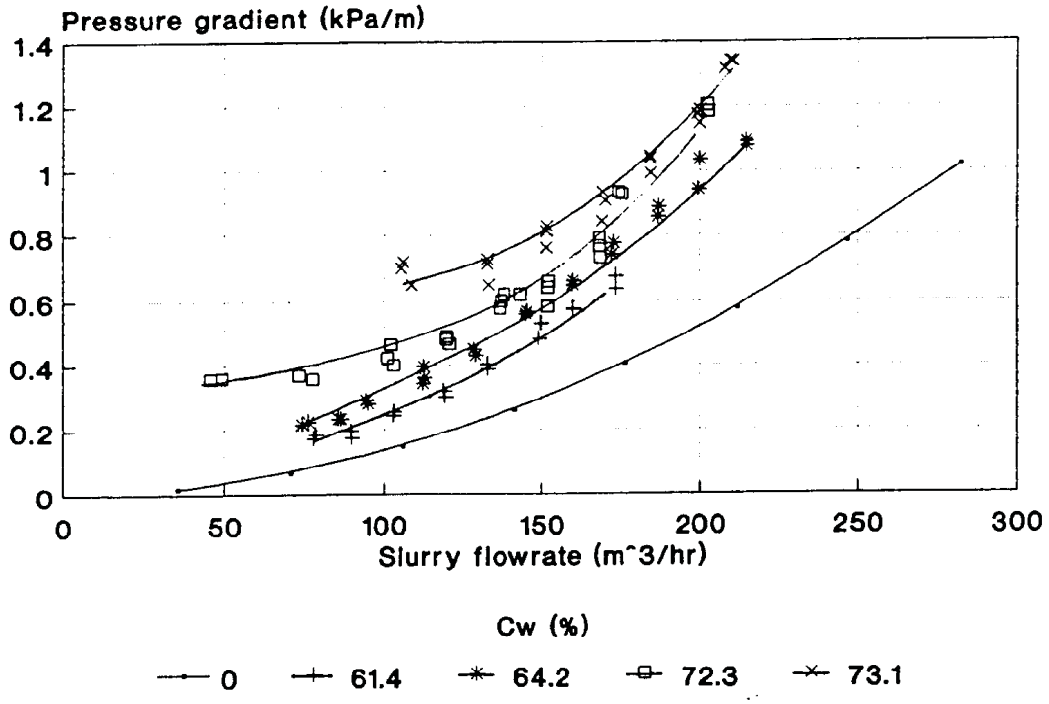

Figure 9.5 Slurry friction gradients (D = 158mm)

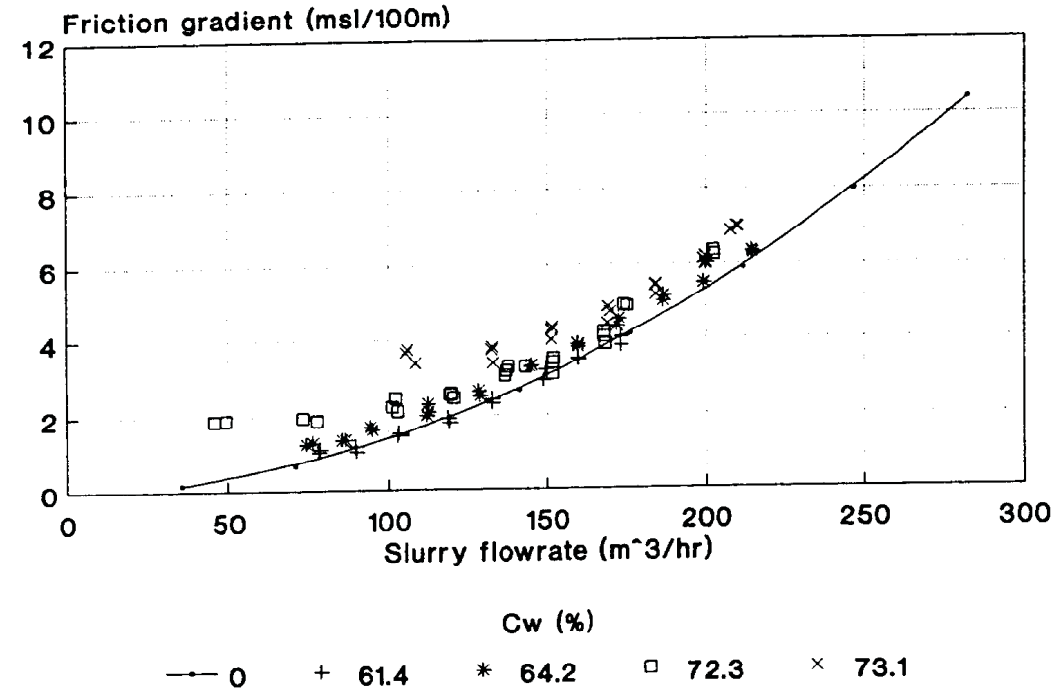

Figure 9.6 Slurry friction gradients (D = 158mm)

The deposit velocities for C_w = 61,4 and 64,2% appear to be in the region of 1,12 - 1,15 m/s in the 158 mm pipeline which is the same as the 52 mm pipeline. An increase in concentration from 64,2% to 72,3% and 73,1% increases the critical deposit velocity to about 1,25 m/s and 1,69 m/s respectively.

Table 9.2 Deposition and Saltation Flowrate Characteristics

		Flowrate (m^3/hr)					
Test	C_w %	Pipe Size (mm)	Black Streaks Along Bottom	Salta-tion	Salta-tion	Slow Moving Bed	Sta-tionery Bed
B	47,3	52	15,33 (2,01)	13,02 (1,70)		11,38 (1,49)	9,95 (1,30)
C	60,8	52	11,82 (1,55)	10,93 (1,43)	10,12 (1,32)	8,76 (1,15)	8,33 (1,09)
D	65,98	52	12,62 (1,65)	11,96 (1,56)	10,68 (1,40)	9,21 (1,20)	7,70 (1,01)
E	64,15	158	128,5 (1,82)	112,5 (1,59)	94,8 (1,34)	85,64 (1,21)	76,09 (1,08)
F	61,43	158	119,4 (1,69)	103,2 (1,46)	89,6 (1,27)	79,59 (1,13)	77,77 (1,10)
G	72,3	158		136,8 (1,94)	120,0 (1,70)	101,90 (1,44)	74,73 (1,06)
H	73,1	158		169,6 (2,40)	151,2 (2,14)	132,5 (1,88)	105,3 (1,49)

( ) The values in brackets indicate the equivalent velocity for the full cross-sectional area of each pipe.

The flow at a concentration above 72% is marked by an irregular wavy pattern in the sight glass, even at velocities higher than the critical deposit velocity. The increase in deposit velocity at these high concentrations

would appear to be due to the hindered particle settling velocity of the individual particles as the concentration approaches the maximum measured bed density of 79% by mass. This results in the bed settling en masse rather than allowing the coarser particles to settle first in a gradual progression.

The skewed velocity distribution that could be observed at these higher concentrations is also possibly responsible for the biased result.

To categorise the type of rheology a series of rheological tests were conducted. Each rheological test was conducted with a sample taken from the pipeline test. The rheological test was conducted at the same mass concentration as the pipeloop tests from which the sample was taken.

The fact that samples were taken from each pipeloop test indicated that particle degradation could play a role in the rheological response. It is clear from the size analysis recorded that degradation had occurred (Table 9.3). These results are illustrated in Fig. 9.7.

Table 9.3 Tails 14 Size distributions

Size (μm)	Cumulative Percentage (%)				
	Unpumped	Test B	Test D	Test E	Test G
600	100,0	100,0	100,0	100,0	100,0
493	97,7	97,5	98,1	98,5	98,2
404	95,0	94,4	95,7	96,5	95,9
301	86,4	83,9	87,5	88,9	88,1
203	62,6	54,5	63,4	65,3	65,7
151	43,1	32,4	44,0	46,1	46,9
102	25,5	15,7	27,4	29,3	29,9
83,4	20,3	11,8	22,7	24,4	24,9

Table 9.3 continued

Size (μm)	Cumulative Percentage (%)				
	Unpumped	Test B	Test D	Test E	Test G
68,5	16,7	9,4	19,5	21,0	21,4
56,2	14,1	8,0	17,1	18,4	18,7
41,8	11,3	6,5	14,4	15,5	15,6
31,1	9,2	5,5	12,2	13,1	13,0
21,0	7,2	4,4	9,9	10,5	10,2
10,5	4,6	2,9	6,6	6,9	6,4
5,27	2,9	1,9	4,2	4,3	4,0
$\varnothing_{max\ 1}$ (%)	73,4				
$\varnothing_{max\ 2}$ (%)	73,8	70,3	75,6	75,8	75,7

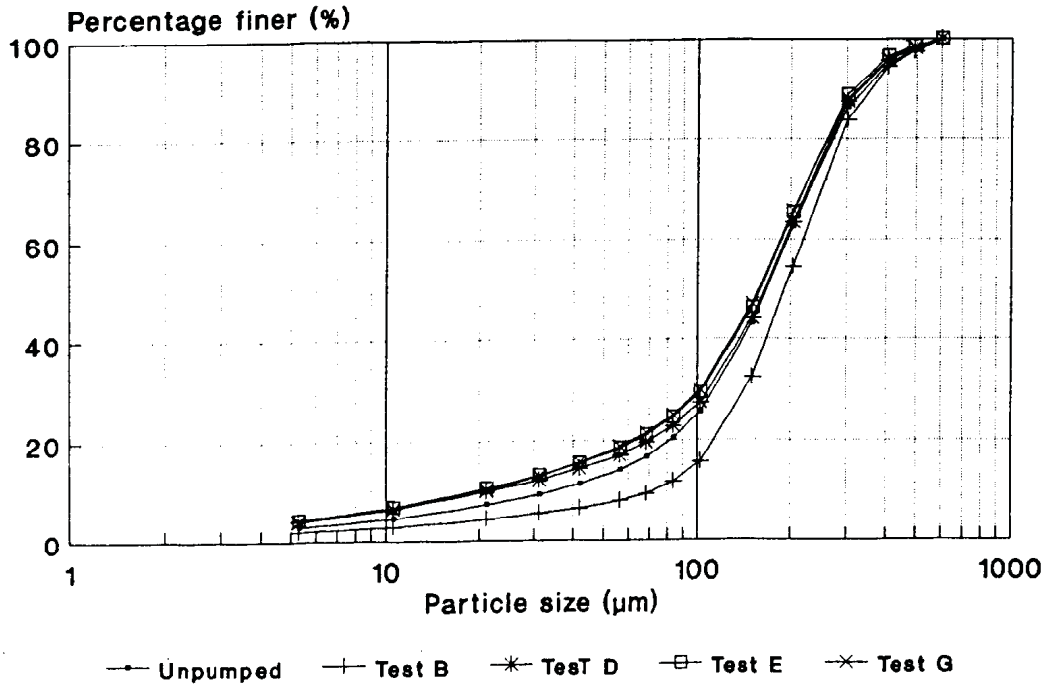

Figure 9.7 Tailings 14 size distributions

It should be noted that the above analysis are for samples sieved through a 300 μm screen. The Malvern analyses nevertheless indicates the presence of 12 - 16% between the sizes of 600 and 300 μm. This discrepancy can be attributed to the difference in the measurement techniques employed. The presence of the sieved portion should nevertheless be considered when analyzing these results.

The comparative rheogram is illustrated in Fig. 9.8. The experimental results indicate the presence of small yield stresses for all the tests, and the characteristics of a generalized Bingham fluid are prevalent for all the tests.

The rheogram for test F, C_w = 61,43% is slightly higher than for test C, C_w = 61,76%. This can be expected as the tailings product had broken down during the pipeline testwork resulting in a finer distribution. This change in distribution is indicated by the trends shown in Section 7.

The experimental curves were subjected to a least squares regression analysis to determine the best fit for the results. The models fitted are given in Table 9.4 together with the strain rate range over which the models were fitted.

Table 9.4 Rheological models fitted to the tails 14 slurries

Test	C_w (%)	Model fitted (Pa)	Applicable strain rate range (1/s)
C	61,76	$\Gamma_w = ,76 + ,0165\ S^{,993}$	$30 < S < 266$
D	65,98	$\Gamma_w = 1,01 + ,0267\ S^{,999}$	$27 < S < 264$
E	64,15	$\Gamma_w = ,71 + ,0355\ S^{,886}$	$27 < S < 269$
F	61,43	$\Gamma_w = ,76 + ,0189\ S^{,981}$	$29 < S < 211$
G	72,26	$\Gamma_w = 1,01 + ,416\ S^{,727}$	$27 < S < 544$

The experimental results utilized for the fitting of the models are included in Appendix X.

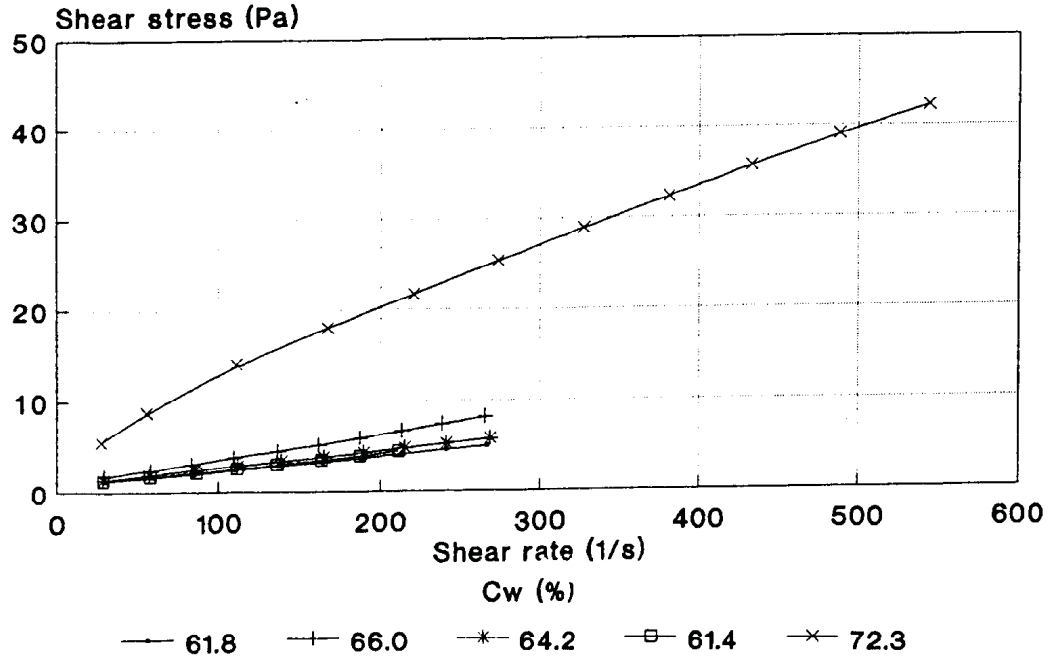

Figure 9.8 Comparative tailings 14 slurry rheogram

A plot of constant shear curves (Fig. 9.9) for increasing concentration indicates an asymptotic increase in the wall stress values in the region of C_w = 66 - 70%. The maximum bed density was measured to occur at C_w = 79%.

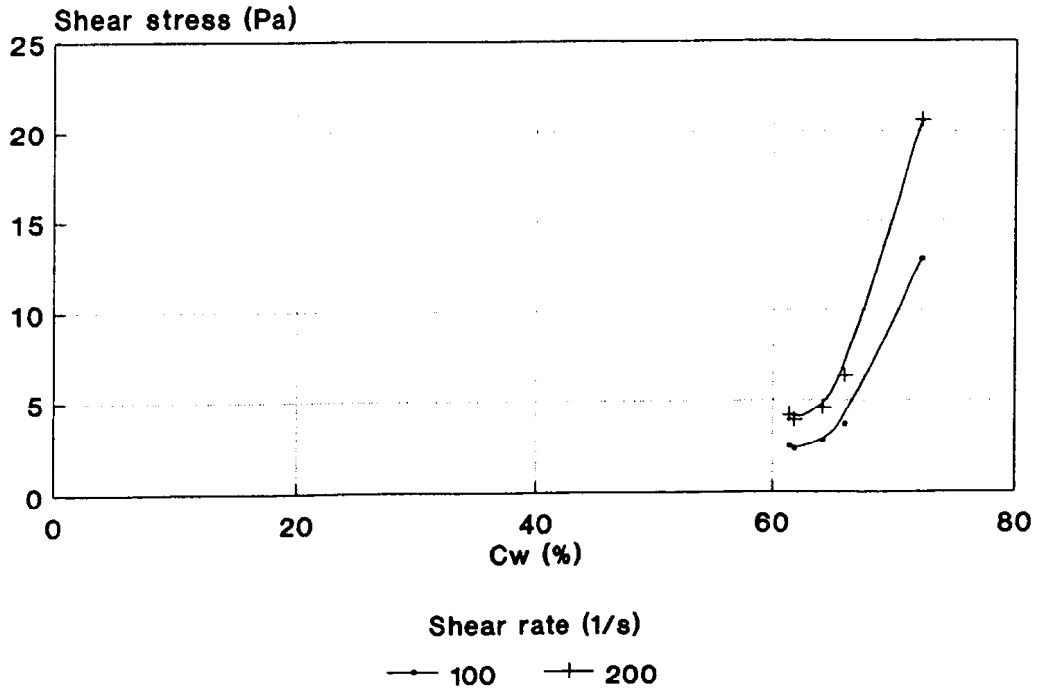

Figure 9.9 Constant shear rate diagram

As the results of the various slurries are to be compared against each other, the various prediction methods for settling slurries discussed in Section 5.5 and 6 are applied to these results.

The accurate prediction of the pressure gradient of a mixed flow regime, settling slurry is a difficult task as no universal correlation has yet been derived that will satisfy all slurries. This is due to the complexity of two phase flow, and the lack of understanding of the micro behavior of the slurry within the confines of the pipe-line.

A number of methods have been proposed for mixed flow regimes. The methods applied to the tails 14 slurries in this section are included in the following Table.

Table 9.5 Prediction formuli for the flow of mixed regime slurries

Method	Reference
Wasp	Section 5.52
Modified Wasp	Section 6.4.4
i_w * r.d.	
Lazarus	Section 5.56
Modified Lazarus	Section 9.2

The results from the various predictions are included in the following Tables.

Table 9.6 Pressure Gradient Predictions for a C_w = 61,76% slurry flowing in a 52 mm pipeline

Velocity (m/s)	Pressure Gradient (kPa/m)					
	Average Experimental	Wasp	Modified Wasp (Pseudo-plastic rheology)	i_w x r.d.	Lazarus	Modified Lazarus
1,0	,70	,718	,581	,387	,605	,605
1,5	,91	1,022	,990	,826	1,013	1,013
2,0	1,42	1,576	1,541	1,425	1,469	1,469
2,5	2,12	2,320	2,189	2,181	2,181	2,181
3,0	2,98	3,597	2,939	3,096	3,096	3,096

Table 9.7 Pressure Gradient Predictions for a C_w = 65,98% slurry flowing in a 52 mm pipeline

Velocity (m/s)	Pressure Gradient (kPa/m)					
	Average Experimental	Wasp	Modified Wasp (Pseudo-plastic rheology)	i_w x r.d.	Lazarus	Modified Lazarus
1,0	,73	,70	,684	,406	,638	,676
1,5	1,03	1,097	1,259	,868	1,071	1,135
2,0	1,60	1,739	1,966	1,496	1,551	1,644
2,5	2,40	2,576	2,789	2,291	2,292	2,429
3,0	3,32	3,925	3,744	3,252	3,251	3,445

Table 9.8 Pressure Gradient Predictions for a C_w = 61,4 slurry flowing in a 158 mm pipeline

Velocity (m/s)	Pressure Gradient (kPa/m)					
	Average Experimental	Wasp	Modified Wasp (Pseudo-plastic rheology)	i_w x r.d.	Lazarus	Modified Lazarus
1,0	,15	,515	,167	,114	,337	,336
1,5	,26	,447	,336	,251	,365	,363
2,0	,46	,542	,558	,441	,539	,537
2,5	,69	,728	,833	,684	,719	,714
3,0	,99	,984	1,158	,977	,981	,977

Table 9.9 Pressure Gradient Predictions for a C_w = 64,2 slurry flowing in a 158 mm pipeline

Velocity (m/s)	Pressure Gradient (kPa/m)					
	Average Experimental	Wasp	Modified Wasp (Pseudo-plastic rheology)	i_w x r.d.	Lazarus	Modified Lazarus
1,0	,23	,453	,168	,117	,357	,369
1,5	,32	,422	,330	,259	,377	,390
2,0	,52	,542	,541	,456	,558	,577
2,5	,78	,748	,800	,705	,755	,781
3,0	1,10	1,022	1,105	1,008	1,008	1,042

Table 9.10 Pressure Gradient Predictions for a C_w = 72,26% slurry flowing in a 158 mm pipeline

Velocity (m/s)	Pressure Gradient (kPa/m)					
	Average Experimental	Wasp	Modified Wasp (Pseudo-plastic rheology)	i_w x r.d.	Lazarus	Modified Lazarus
1,0	,37	,234	,185	,130	,412	,475
1,5	,45	,361	,414	,286	,423	,487
2,0	,56	,579	,634	,503	,624	,719
2,5	,88	,867	,884	,780	,846	,975
3,0	1,26	1,286	1,172	1,115	1,115	1,285

In general all the original models used above use the friction factor of the original fluid, viz water as the base of their predictions. The influence of the solids is then added to the water friction factor, and the

overall pressure gradient is based on this derived friction factor. It is however clear from the experimental results illustrated in terms of $m_{sl}/100$ m that the overall slurry friction factor is less then the friction factor of water for the lower concentration slurries.

The prediction methods using f_{water} as the base could therefore be expected to result in higher predicted values of the friction gradient. From this observation it would appear that two options are available. The first involves using the appropriate rheology while the second involves modifying the results by multiplying the derived friction factor by an experimentally derived constant, based on one or more of the slurry parameters.

The results of these two options are also included in Tables 9.6 - 9.10. The pseudoplastic rheology obtained from the comparative rheogram (Table 9.4) is utilized in the Modified Wasp method, while the factor $K = \sqrt{\frac{C_v}{34,84}}$ is applied to the f_m/f_b derived from the Lazarus method. These results are more representative of the measured results than the original methods utilized.

It is possible to modify any of the other methods utilized, but this would result in predictions deviating from the original premise utilized in deriving these equations in that the overall friction factor is based on the friction factor of water.

As the only method that can result in lower overall friction factors is based on the friction factor derived from the rheology of the slurry it would appear that this method is the best method to utilize.

The prediction of the critical deposit velocity is also required to compare the results of this slurry with the results of the other settling slurries tested in this chapter.

The methods used to predict the critical velocity are included in the following Table (9.11).

Table 9.11 Deposit velocity prediction formuli

Method	Reference	Equation
Durand	(79)	$V_D = F_L \sqrt{2gD(s-1)}$
Wasp 1	Section 5.52	
Wasp 2	Section 5.52	
Newitt	(40)	$V_D = .5(40\ \phi_v\ Dg\ (s-1)/\sqrt{C_D})$
Modified Durand	(124)	$V_D = F_L \sqrt{2gD(S-S_m)}$
Thomas	(87)	$V_D = 9,0\ [g\eta\ \frac{(s-1)}{\rho}]^{.37}\ [\frac{Dp}{\eta}]^{.11}$

The resulting predictions are included in the following Table (9.12).

Table 9.12 Predicted deposition velocities

		Deposition velocity (m/s)						
C_w (%)	ID (mm)	Experimental deposition velocity	Durand	Modified Durand	Wasp 1	Wasp 2	Thomas*	Newitt**
47,3	52	1,40	1,44	1,40	1,31	1,03	,83	1,24
61,8	52	1,12	1,46	1,27	1,41	1,03	,94	1,53
66,0	52	1,11	1,45	1,22	1,44	1,03	1,00	1,62
61,4	158	1,12	2,58	2,36	2,06	1,49	1,06	2,66
64,2	158	1,15	2,55	2,36	2,08	1,49	1,10	2,76
72,3	158	1,25	2,52	2,19	2,16	1,49	1,28	3,08

* Viscosity values used are based on minimum μ_{app} obtained from viscosity tests.

** C_D is based on the particle falling in the slurry.

As is shown there is a wide range in both the experimental results and the predictions. The experimental values in general decrease with an increase in concentration as the particle settling becomes more hindered. The exception is the experimental values obtained for concentrations larger than 70%.

It is possible to obtain a predicted value that corresponds better to the experimental results, by modifying the predicted values with a constant based on the pipeline diameter and slurry concentration.

9.3 Tails 15

The slurry tests were conducted in 200 mm NB rubber lined (ID = 192 mm) pipes. Prior to, during and after, the slurry tests, water was pumped through the pipeline to detect any possible changes of the pipe internal surfaces as a result of wear.

The friction gradients for the various water tests conducted are included in Appendix Y and illustrated in Fig. 9.10. An iterative analysis of the experimental data resulted in the relative roughness of 0,0001 for the rubber lined pipe. The limited scatter of the experimental results are indicative of little or no wear during the test period.

To ensure reproductibility and to establish the degree of degradation during the tests, two samples for size analysis tests were taken before and after the tests. The results are included in Table 9.13 and illustrated in Fig. 9.11. Samples 3 and 4 were taken prior to the pump tests while 1 and 2 during the pump tests. As shown by the calculated d_{50} values, the particle size remained fairly constant during the test with only a small amount of degradation being recorded from the analysis.

Furthermore the size analysis indicates that the bulk of the material lies between 180 and 425 μm, indicating a narrow size distribution. The relatively coarse nature of the tailings indicated that a minimum deposition velocity could be expected. The tailings were too coarse for any preliminary rheological characterization.

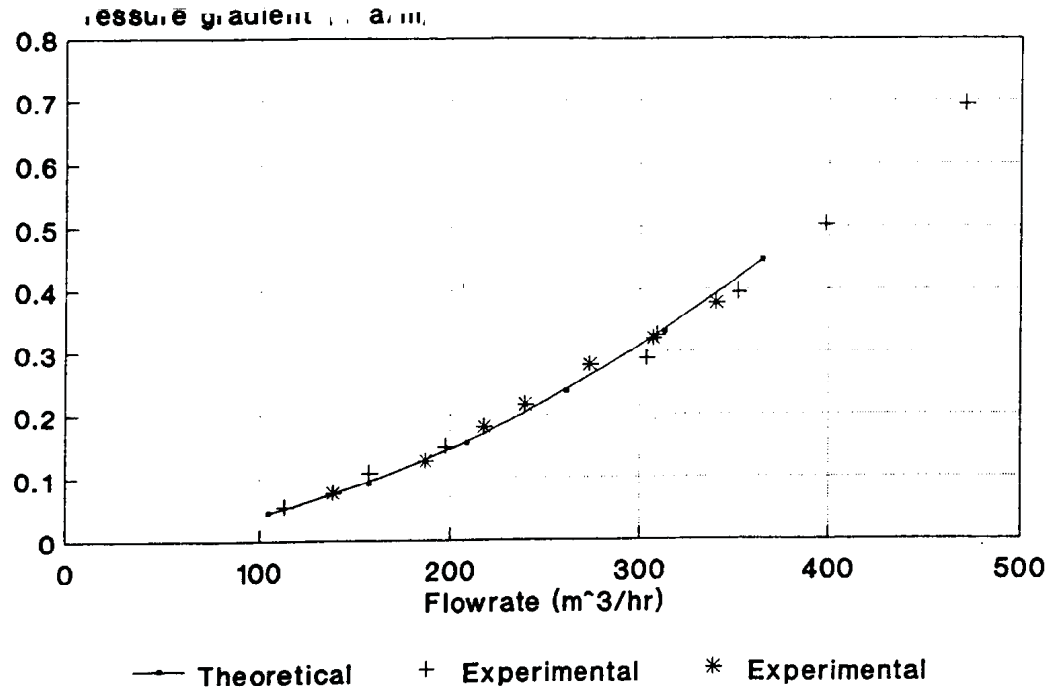

Fig. 9.10 Clean water friction gradients for the rubber lined pipeline (ID = 192mm)

Table 9.13 Tail 15 size distribution analysis

Size (mm)	Cumulative percentage passing (%)			
Sample no	1	2	3	4
1,16	100,0	100,0	100,0	100,0
0,60	98,4	98,7	98,5	98,8
0,425	93,9	94,5	91,6	91,9
0,300	66,2	66,9	66,2	63,6
0,180	8,2	10,9	11,0	10,4
0,150	3,0	4,4	5,6	5,4
0,106	0,53	0,5	1,3	1,1
0,075	0,39	0,20	0,06	0
0,063	0,11	0,08	0,03	
0,053	0,05	0,05		
0,045	0,02	0,02		
d_{50} (mm)	0,267	0,264		
$\varnothing_{max\ 1}$ (%)	64,9			
$\varnothing_{max\ 2}$ (%)	65,0			

Pipeline tests were conducted at concentrations (C_w's) of 29,7, 44,5 and 60,7%. The experimental data is illustrated in terms of kPa/m in Fig. 9.12 and in terms of m_{sl}/100m in Figure 9.13.

The curves are typical of a single sized heterogeneous slurry, displaying a minimum friction gradient in the region of the deposition velocity and asymptoting towards the clean water curves at higher velocities.

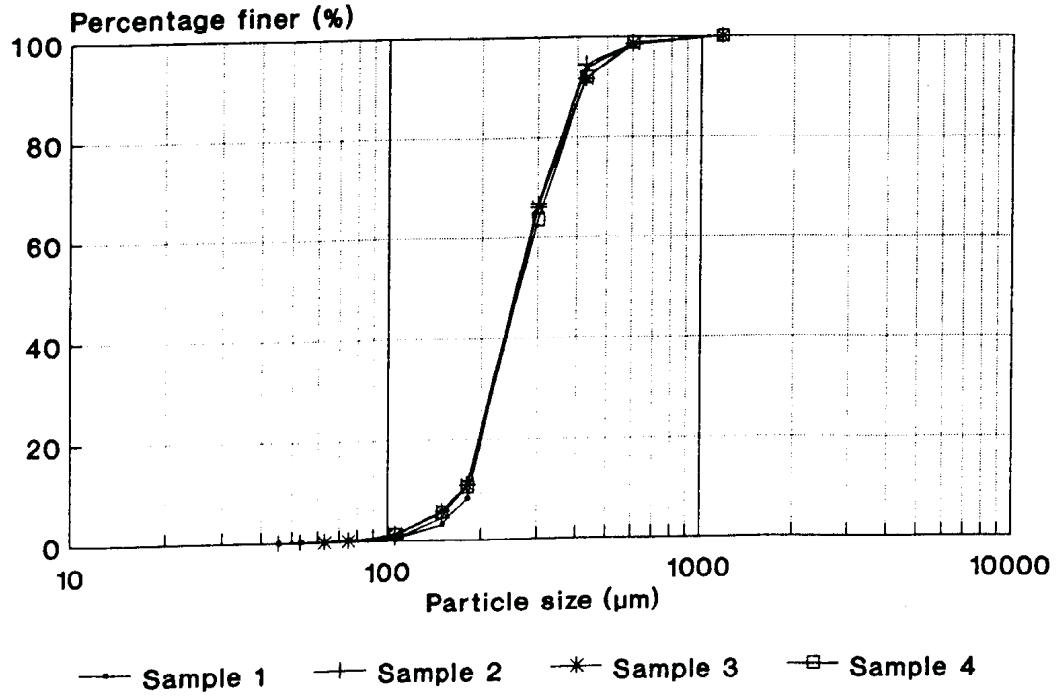

Fig. 9.11 Tailings 15 Size distribution

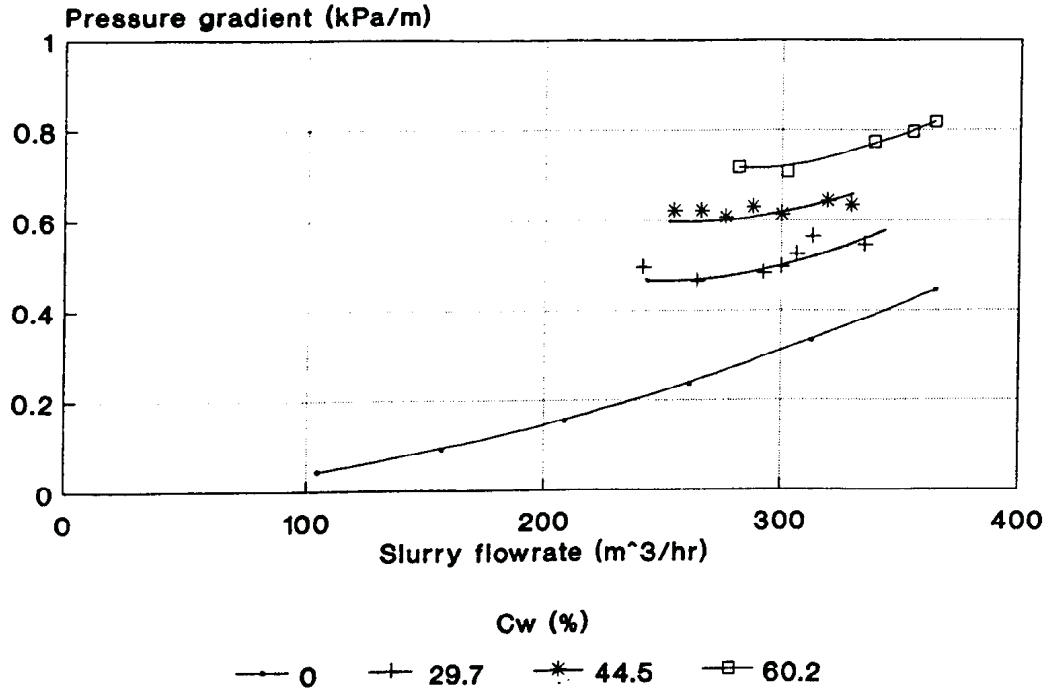

Fig 9.12 Tails 15 Friction Gradients (Rubber)

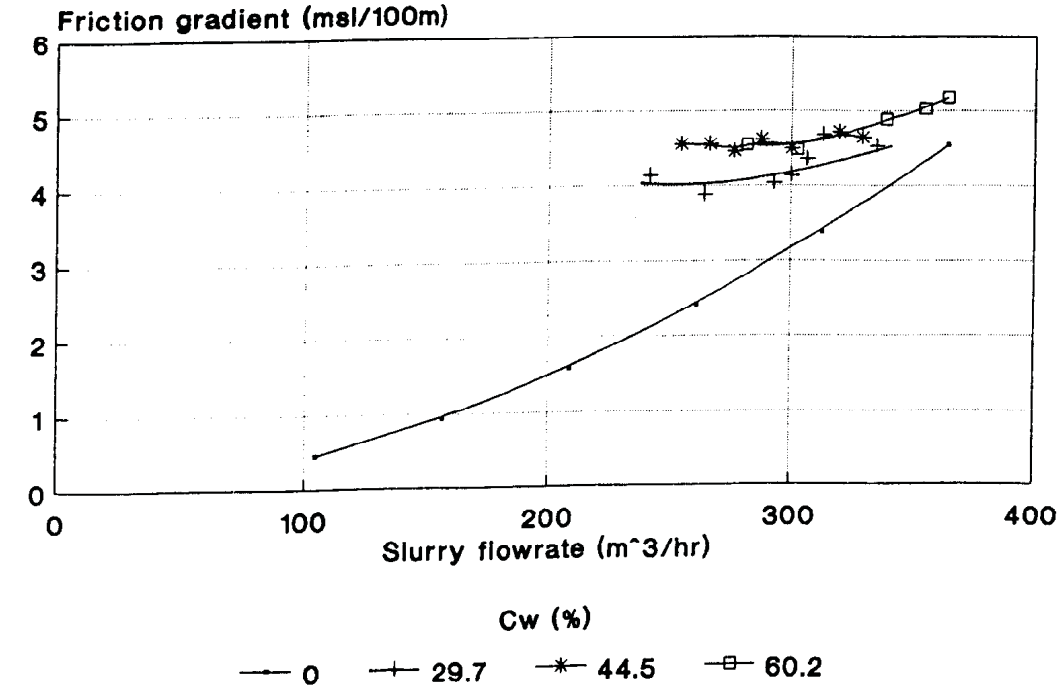

Fig. 9.13 Tails 15 Friction Gradients (Rubber)

The deposition velocity range observed through a 212 mm ID viewing section for the tailings slurry is given in the following Table:

Table 9.14 Deposition velocity range for the tailings slurries

C_w (%)	Deposition range (m^3/hr)	m/s
29,7	293 - 312	2,31 - 2,46
44,5	288 - 319	2,27 - 2,51
60,2		

The single sized distribution, the relative coarseness of the particles, and the observed performance characteristics of these slurries, would indicate the applicability of models simulating mixed regime/ heterogeneous regime type slurries.

The tailings product used in these tests is substantially coarser than those tested in Section 7. (d_{50} = 264 μm as apposed to (tails 8) d_{50} = 107 μm). As tails 8 displayed Newtonian like rheological characteristics it can be expected that tails 15 would have similar characteristics with the viscosity characteristics being a function of the volume concentration and the maximum packing density.

The correlations thus utilized to approximate the friction gradients include the Wasp and Lazarus correlation (Table 9.5). The friction gradients derived are included in the following Tables.

Table 9.15 Pressure Gradient predictions for a C_w = 29,7% slurry flowing in a 192 mm rubber lined pipe

Velocity (m/s)	Pressure Gradient (kPa/m)			
	Average Experimental	Wasp	Lazarus	Durand
1,5				
2,0		,506	,301	,567
2,5	0,48	,507	,401	,557
3,0	0,52	,556	,506	,593
3,5	0,60	,641	,619	,666
4,0		,754	,734	,765

Table 9.16 Pressure Gradient predictions for a C_w = 44,5% slurry flowing in a 192 mm rubber lined pipe

Velocity (m/s)	Pressure Gradient (kPa/m)			
	Average Experimental	Wasp	Lazarus	Durand
1,5				
2,0		,632	,311	
2,5	0,61	,605	,414	,778
3,0	0,64	,641	,523	,774
3,5	0,70	,727	,639	,818
4,0		,848	,792	,896

Table 9.17 Pressure Gradient predictions for a C_w = 60,7% slurry flowing in a 192 mm rubber lined pipe

Velocity (m/s)	Pressure Gradient (kPa/m)			
	Average Experimental	Wasp	Lazarus	Durand
1,5				
2,0		,771	,327	
2,5	0,72	,706	,435	1,048
3,0	0,74	,732	,549	1,023
3,5	0,84	,818	,712	1,028
4,0		,915	,912	1,078

The Wasp prediction is based on the Durand coefficient K of 82 (eqn 5.113) while the viscosity values utilized are based on an iterative procedure such that the predicted friction gradients coincide with the experimental results. The values used are compared with the values obtained from some of the methods listed in Table 5.1, in Table 9.18.

Table 9.18 Comparison of derived viscosity values for the tails 15 slurry

Cw (%)	Relative viscosity				
	Derived	Vand Roscoe Brinkman	Vand	Roscoe	Frankel Arcivos
29,7	1,67	1,45	1,46	1,64	1,50
44,5	2,56	1,94	1,97	2,56	2,39
60,2	3,5	3,09	3,21	5,40	4,21

The Durand equation is based on the original Durand equation

$$\phi = K\Omega^{-m} \qquad (5.112)$$

where $$\Pi = \frac{V^2}{gD} \quad \frac{\sqrt{C_D}}{(s-1)} \qquad -(9.1)$$

and $$K = 81$$

The Wasp prediction using the derived viscosity values fits the data best. The Lazarus method although assymptoting towards the experimental results at the higher velocities underpredicts the friction gradients.

The Durand equation although derived from test work on single sized slurries overpredicts the friction gradients. Other researchers have shown that different data can be correlated with the basic Durand equation using different values of K and m[125].

The friction gradient results (Fig. 9.13) indicate that the friction gradient assymptotes towards the water curve, which would indicate that a prediction method based on the water based friction gradient is applicable with this tailings product.

The prediction of the critical deposit velocities is based on the equations listed in Table 9.11. The resulting predictions are included in the following Table.

Table 9.19 Predicted deposition velocities

C_w (%)	Deposition velocity (m/s)						
	Pipe I.D. (mm)	Experimental V_D	Durand	Modified Durand	Wasp	Wasp	Newitt
19,7	212	2,39	2,80	2,80	1,71	1,64	1,72
44,5	212	2,39	3,00	2,98	2,07	1,64	2,86
60,7	212	2,50	2,99	2,98	2,26	1,64	3,60

As shown by the above values there is a wide range in the predicted values. The Durand and modified Durand approximating the safest methods to use for predicting the critical deposit velocity. It should be noted that Durand's method is based on experimental work with single sized sand slurries and it can therefore be expected that this method best approximates the experimental results.

The coarse material slurry formed from the tailings 15 product is thus characterized by mixed/heterogeneous type prediction formula. The characteristic is also confirmed by the changing concentration profile that could be observed through the perspex sight glass at the different flow velocities.

The highest concentration transported corresponds to approximately 65% of the maximum packing density. Care should be exercised with higher concentrations of slurries of this size, as restart and the formation of unpumpable plugs, becomes a problem at the higher concentrations.

9.4 Tails 16

The tests on the Tails 16 slurries were conducted in a 49mm pipeline as this pipe size represented the size to be used on the mine backfill system. The design concentration for the system was 1,60 but fluctuations in the backfill plant, and the possibility that coarse aggregate would be introduced into the slurry resulted in tests being conducted from C_w = 35% to C_w = 63%.

The size distribution of the unpumped material and of samples taken during the various tests are tabled in Table 9.20 and illustrated in Fig. 9.14.

Table 9.20 Size analysis of the Tails 16 Samples

Size (mm)	Cumulative percentage passing (%)					
	Un-pumped	After Test 3	After Test 4	After Test 5	After Test 6	After Test 7
0,833	99,9	100,0	100,0			
0,589	99,5	93,3	94,7	96,5	99,6	97,7
0,417	98,4	92,8	94,3	96,3	99,1	97,0
0,295		91,4	93,0	94,8	97,8	95,5
0,208	94,2		76,6			
,147	47,8	64,5	56,8	62,2	70,2	63,8
,104	17,8	30,8	43,9	27,4	34,1	22,7
,074	3,9	10,4	20,8	13,5	27,0	17,2
$\varnothing_{max\ 1}$ (%)	66,0					
$\varnothing_{max\ 2}$ (%)	65,9					

The solids specific gravity utilized for these tests is 2,68. The experimental curve for water flowing through the Schedule 80, 49 mm ID pipe is illustrated in Fig. 9.15. Successive iterations of the Colebrook-White equation revealed that a roughness ratio of k/d = 0,0009 fitted the experimental results.